The 2010 IEEE/RSJ International Conference on
Intelligent Robots and Systems
October 18-22, 2010, Taipei, Taiwan

Comparison of 3-PPR Parallel Planar Manipulators Based on their Sensitivity to Joint Clearances

Nicolas Binaud, Stéphane Caro, Shaoping Bai and Philippe Wenger

Abstract— **In this paper, 3-PPR planar parallel manipulators with Δ- or U-shape base are compared with respect to their workspace size and kinematic sensitivity to joint clearances. First, the singularities and workspace of a general 3-PPR planar parallel manipulator are analyzed. Then, an error prediction model applicable to both serial and parallel manipulators is developed. As a result, two nonconvex quadratically constrained quadratic programs are formulated in order to find the maximum reference-point position error and the maximum orientation error of the moving-platform for given joint clearances. Finally, the contributions of the paper are highlighted by means of a comparative study of two manipulators.**

I. INTRODUCTION

Parallel manipulators are mechanisms that consist of two platforms, one fixed and the other movable, connected by multiple kinematic chains. Compared with serial industrial manipulators, parallel manipulators have advantages of high stiffness, high accuracy, high payload-mass ratio. However, an obvious drawback is the small workspace.

The kinematics and design of Planar Parallel Manipulators (PPMs) have been extensively studied. Gosselin and Angeles studied the optimum kinematic design of 3-RRR PPMs [1]. Ur-Rehman et al. focused on the multiobjective design optimization of 3PRR PPMs [2]. The singularities of PPMs were analyzed by means of screw theory in [3]. The actuation with a redundant degree of freedom was investigated in [4]. Merlet reported the direct kinematics of planar robot [5].

In the design of parallel manipulators, most designs adapt a symmetric topology. In the case of planar parallel manipulators with three legs, a symmetric topology implies that the base and mobile platforms are equilateral and the three legs are identical. The design with a symmetric topology simplifies the manufacture and assembly. However, a symmetrical design may not be optimal in terms of some kinematic performance. A 3-PPR PPM with a U-shape base was proposed in [6] and a prototype is shown in Fig. 1(a).

Among the most important sources of errors, we find manufacturing errors, assembly errors, compliance in the mechanical architecture, resolution of the servoactuators, backlash in the reductors, and clearances in the joints. As indicated in [7], [8], the errors due to manufacturing, assembly and compliance can be compensated through calibration and model-based control. Joint clearances, on the contrary, exhibit low repeatability, which generally makes their compensation difficult. For this reason, the focus of this paper is the impact of joint clearances on the pose errors of the moving platform of 3-PPR PPMs with Δ- or U-shape base.

The paper is organized as follows. First, the two manipulators under study are presented. Then, their kinematic model is derived in order to analyze their workspace and singularities. Finally, an error prediction model is developed and the contributions of the paper are highlighted by means of a comparative study of two 3-PPR PPMs with a Δ- and a U-shape base, respectively.

II. MANIPULATORS UNDER STUDY

Here and throughout this paper, R, P and P denote revolute, prismatic and actuated prismatic joints, respectively. Figure 1(a) illustrates the prototype of a 3-PPR PPM with a U-shape base introduced in [6] while Fig. 1(b) shows a 3-PPR PPM with a Δ-shape base. Both the manipulators contain a Δ-shape moving platform (MP) connected to the base by means of three identical kinematic chains, each one being composed of two orthogonal prismatic joints and a revolute joint. Notice that the second prismatic joint of each chain is actuated. The parameterization of the 3-PPR PPM is illustrated with Fig. 2. $\mathscr{F}_b$ and $\mathscr{F}_p$ are the base and the moving platform frames of the manipulator. In the scope of this paper, $\mathscr{F}_b$ and $\mathscr{F}_p$ are supposed to be orthogonal. $\mathscr{F}_b$ is defined with the orthogonal dihedron $(\vec{O}x, \vec{O}y)$, point O being its center and $\vec{O}x$ parallel to segment A_1A_2. Likewise, $\mathscr{F}_p$ is defined with the orthogonal dihedron $(\vec{P}X, \vec{P}Y)$, point P being its center and $\vec{P}X$ parallel to segment C_1C_2. The manipulator MP pose, i.e., its position and its orientation, is determined by means of the Cartesian coordinates vector $\mathbf{p} = [p_x, p_y]^T$ of operation point P expressed in frame $\mathscr{F}_b$ and angle ϕ, namely, the angle between frames $\mathscr{F}_b$ and $\mathscr{F}_p$.

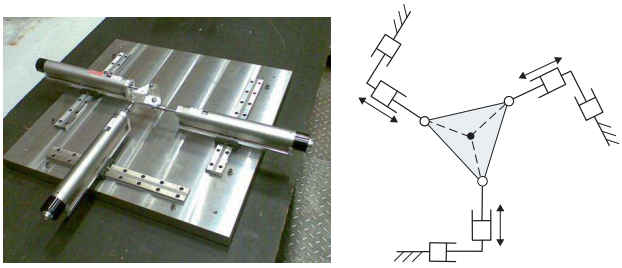

(a) (b)

Fig. 1. 3-PPR PPMs with (a) a U- and (b) a Δ-shape base

N. Binaud, S. Caro and P. Wenger are with the Institut de Recherche en Communications et Cybernétique de Nantes, UMR CNRS 6597, 1 rue de la Noë, 44321 Nantes, France, nicolas.binaud@irccyn.ec-nantes.fr

S. Bai is with the Department of Mechanical Engineering, Aalborg University, Denmark, shb@ime.aau.dk

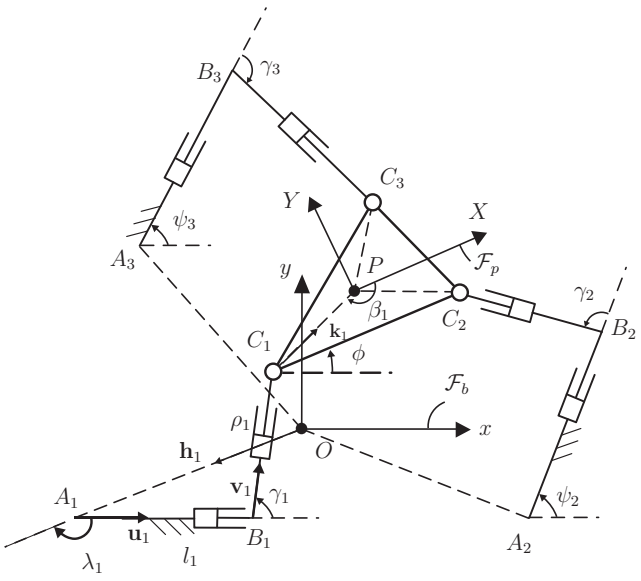

Fig. 2. Parameterization of a 3-P$\underline{\text{P}}$R PPM

III. KINEMATIC ANALYSIS

A. Singularities

From the closed-loop kinematic chains $O-A_i-B_i-C_i-P-O$, $i=1,\ldots,3$ depicted in Fig. 2, the position vector $\mathbf{p}$ of point P can be expressed in $\mathscr{F}_b$ as follows,

$$\mathbf{p}=\begin{bmatrix} p_x \\ p_y \end{bmatrix}=\mathbf{a}_i+(\mathbf{b}_i-\mathbf{a}_i)+(\mathbf{c}_i-\mathbf{b}_i)+(\mathbf{p}-\mathbf{c}_i) \quad (1)$$

$\mathbf{a}_i$, $\mathbf{b}_i$ and $\mathbf{c}_i$ being the position vectors of points A_i, B_i and C_i expressed in $\mathscr{F}_b$. Equation (1) can also be written as,

$$\mathbf{p}=a_i\mathbf{h}_i+l_i\mathbf{u}_i+\rho_i\mathbf{v}_i+c_i\mathbf{k}_i \quad (2)$$

where a_i is the distance between points O and A_i, l_i is the distance between points A_i and B_i, ρ_i is the distance between points B_i and C_i, c_i is the distance between points C_i and P, $\mathbf{h}_i$ is the unit vector $\vec{OA_i}/\|\vec{OA_i}\|_2$, $\mathbf{u}_i$ is the unit vector $\vec{A_iB_i}/\|\vec{A_iB_i}\|_2$, $\mathbf{v}_i$ is the unit vector $\vec{B_iC_i}/\|\vec{B_iC_i}\|_2$ and $\mathbf{k}_i$ is the unit vector $\vec{C_iP}/\|\vec{C_iP}\|_2$. Upon differentiation of Eq. (2) with respect to time, we obtain:

$$\dot{\mathbf{p}} = \dot{l}_i\,\mathbf{u}_i+\dot{\rho}_i\,\mathbf{v}_i+c_i\dot{\phi}\,\mathbf{E}\,\mathbf{k}_i \quad (3)$$

with matrix $\mathbf{E}$ defined as

$$\mathbf{E}=\begin{bmatrix} 0 & -1 \\ 1 & 0 \end{bmatrix} \quad (4)$$

$\dot{\mathbf{p}}$ and $\dot{\phi}$ being the position and orientation velocities of the MP. Likewise, $\dot{l}_i$ and $\dot{\rho}_i$ denote the prismatic joint rates. The idle term $\dot{l}_i$ is eliminated by dot-multiplying Eq. (3) with $\mathbf{u}_i^T\mathbf{E}$, thus obtaining

$$\mathbf{u}_i^T\mathbf{E}\dot{\mathbf{p}} = \dot{\rho}_i\,\mathbf{u}_i^T\mathbf{E}\,\mathbf{v}_i-c_i\dot{\phi}\mathbf{u}_i^T\mathbf{k}_i \quad (5)$$

Equation (5) can now be cast in vector form:

$$\mathbf{A}\begin{bmatrix} \dot{\phi} \\ \dot{\mathbf{p}} \end{bmatrix} = \mathbf{B}\begin{bmatrix} \dot{\rho}_1 \\ \dot{\rho}_2 \\ \dot{\rho}_3 \end{bmatrix} \quad (6)$$

with

$$\mathbf{A} = \begin{bmatrix} m_1 & \mathbf{u}_1^T\mathbf{E} \\ m_2 & \mathbf{u}_2^T\mathbf{E} \\ m_3 & \mathbf{u}_3^T\mathbf{E} \end{bmatrix} \quad (7a)$$

$$\mathbf{B} = \mathrm{diag}\begin{bmatrix} \mathbf{u}_1^T\mathbf{E}\mathbf{v}_1 & \mathbf{u}_2^T\mathbf{E}\mathbf{v}_2 & \mathbf{u}_3^T\mathbf{E}\mathbf{v}_3 \end{bmatrix} \quad (7b)$$

and

$$m_i=c_i\,\mathbf{u}_i^T\mathbf{k}_i, \quad i=1,\ldots,3 \quad (8)$$

Notice that $\mathbf{A}$ and $\mathbf{B}$ are the direct and the inverse Jacobian matrices of the manipulator, respectively. We obtain upon multiplication of Eq. (6) by $\mathbf{A}^{-1}$:

$$\begin{bmatrix} \dot{\phi} \\ \dot{\mathbf{p}} \end{bmatrix} = \mathbf{J}\begin{bmatrix} \dot{\rho}_1 \\ \dot{\rho}_2 \\ \dot{\rho}_3 \end{bmatrix} \quad (9)$$

with

$$\mathbf{J} = \mathbf{A}^{-1}\mathbf{B} \quad (10)$$

It turns out that the kinematic Jacobian matrix $\mathbf{J}$ is singular when $\phi\equiv 0[\pi]$ for the 3-P$\underline{\text{P}}$R PPM with U-shape base and when $\phi\equiv\pi/3[2\pi]$ for the 3-P$\underline{\text{P}}$R PPM with a Δ-shape base and an equilateral mobile platform.

B. Workspace

For planar parallel manipulators, the limited workspace is seen in both the small reachable area and low orientational capability. We first look at the reachable area, which is represented by constant-orientation workspace. To get the reachable area geometrically, the inverse kinematic model is used to establish the boundaries of end-effector displacements. Let the moving range of the proximal and distal prismatic joints be $[l_{min},l_{max}]$ and $[\rho_{min},\rho_{max}]$, respectively. The motion constraints on the two joints are thus expressed as

$$l_{min}\le l_i\le l_{max}, \quad \rho_{min}\le\rho_i\le\rho_{max} \quad (11)$$

The workspace of the system is the intersection of the feasible regions of three legs. In the scope of this study, we choose l_{min}=0, l_{max}=280, ρ_{min}=50 and ρ_{max}=300 expressed in [mm]. Besides, let us study the 3-P$\underline{\text{P}}$R PPM, with the geometric parameters given in Table I. λ_i, ψ_i and β_i, $i=1,2,3$, being expressed in [rad] and r_1 and r_2 in [mm] with $r_1=a_1=a_2=a_3$ and $r_2=c_1=c_2=c_3$. Angles γ_i, $i=1,2,3$ are equal to $\pi/2$. Constant-orientation workspaces WS of the two 3-P$\underline{\text{P}}$R PPMs are shown in Figs. 3 and 4. It is apparent that the workspace of the 3-P$\underline{\text{P}}$R PPM with a U-shape base is quite larger than the one of the 3-P$\underline{\text{P}}$R PPM with a Δ-shape base.

IV. ERROR PREDICTION MODEL

A methodology is introduced in this section to obtain the variations in the moving platform pose as a function of joint clearances. Let us assume that the *i*th leg is a serial kinematic chain composed of three links, the first being connected to the base and the third one to the moving-platform. We describe these open kinematic chains mathematically using the Denavit-Hartenberg parameters.

TABLE I

GEOMETRIC PARAMETERS OF THE 3-PPR PPMS UNDER STUDY (LENGTHS EXPRESSED IN [MM] AND ANGLES IN [RAD])

	r_1	r_2	λ_1	λ_2	λ_3	ψ_1	ψ_2	ψ_3	β_1	β_2	β_3
U-shape	224.5	62.5	$\pi/4$	$-\pi/4$	$3\pi/4$	$\pi/2$	$\pi/2$	0	$-5\pi/6$	$-\pi/6$	$\pi/2$
Δ-shape	224.5	62.5	$-5\pi/6$	$-\pi/6$	$\pi/2$	0	$2\pi/3$	$\pi/3$	$-5\pi/6$	$-\pi/6$	$\pi/2$

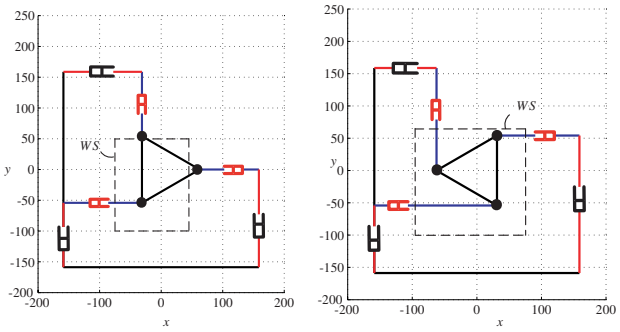

(a) (b)

Fig. 3. Constant-orientation workspace of the 3-PPR PPM with U-shape base: (a) $\phi = \pi/6$, (b) $\phi = \pi/2$

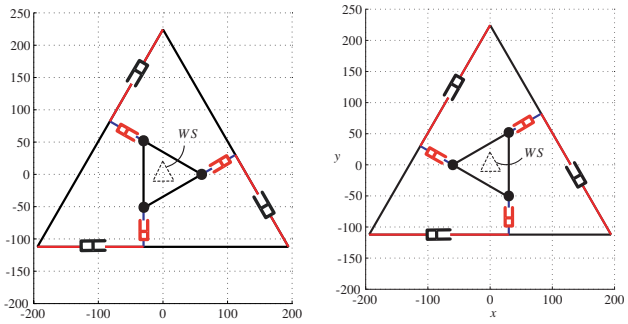

(a) (b)

Fig. 4. Constant-orientation workspace of the 3-PPR PPM with Δ-shape base: (a) $\phi = \pi/6$, (b) $\phi = \pi/2$

A. Parameterization

Let us define frame $\mathscr{F}_{i,j}$, which is attached to the j^{th} link of the i^{th} leg. Moreover, $\mathscr{F}_{i,1}$, $i = 1,\ldots,3$, are the reference frames attached to the fixed base and have the same orientation. $\mathscr{P}_i = \mathscr{F}_{i,3}$, $i = 1,\ldots,3$, are attached to the moving-platform of the 3-PPR PPM. Each frame is related to the previous one by the transformation matrix:

$$\mathbf{S}_{i,j} = \begin{bmatrix} \mathbf{R}_{i,j} & \mathbf{t}_{i,j} \\ \mathbf{0}_3^T & 1 \end{bmatrix} \in \mathrm{SE}(3), \tag{12}$$

which takes $\mathscr{F}_{i,j}$ onto $\mathscr{F}_{i,j+1}$, and where $\mathbf{R}_{i,j} \in \mathrm{SO}(3)$ is a 3×3 rotation matrix; $\mathbf{t}_{i,j} \in \mathbb{R}^3$ points from the origin of $\mathscr{F}_{i,j}$ to that of $\mathscr{F}_{i,j+1}$, and $\mathbf{0}_3$ is the three-dimensional zero vector. Moreover, all frames follow the Denavit-Hartenberg convention [9], so that $\mathbf{S}_{i,j}$ may be expressed as

$$\mathbf{S}_{i,j} = \mathbf{S}_{i,j,\theta}\mathbf{S}_{i,j,b}\mathbf{S}_{i,j,a}\mathbf{S}_{i,j,\alpha}, \tag{13}$$

where

$$\mathbf{S}_{i,j,\alpha} \equiv Rot(X, \alpha_{i,j}), \tag{14}$$

$$\mathbf{S}_{i,j,a} \equiv Trans(X, a_{i,j}), \tag{15}$$

$$\mathbf{S}_{i,j,b} \equiv Trans(Z, b_{i,j}), \tag{16}$$

$$\mathbf{S}_{i,j,\theta} \equiv Rot(Z, \theta_{i,j}), \tag{17}$$

and where $\alpha_{i,j}$, $a_{i,j}$, $b_{i,j}$ and $\theta_{i,j}$ represent the link twist, the link length, the link offset, and the joint angle, respectively. In our case the second prismatic joint is actuated, thus $b_{i,2}$ is a variable. Figure 5 and Table II illustrate the parameterization of the 3-PPR PPM legs.

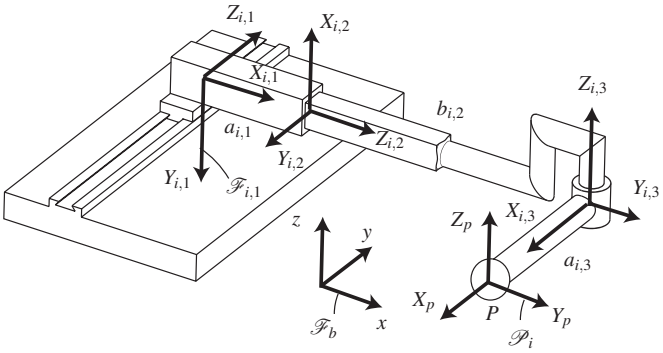

Fig. 5. Denavit-Hartenberg parameters of the 3-PPR PPM's legs

TABLE II

DENAVIT-HARTENBERG PARAMETERS OF THE 3-PPR PPM'S LEGS

	a_i	b_i	α_i	θ_i
$\mathbf{S}_{i,1}$	$a_{i,1}$	0	$-\pi/2$	$-\pi/2$
$\mathbf{S}_{i,2}$	0	$b_{i,2}$	$\pi/2$	$\pi/2$
$\mathbf{S}_{i,3}$	$a_{i,3}$	0	0	$\theta i,3$

B. The Moving-Platform Pose

Thence, the pose of the third link with respect to the fixed frame $\mathscr{F}_{i,1}$ may be expressed as

$$\mathbf{P}_i = \prod_{j=1}^{3} \mathbf{S}_{i,j}, \tag{18}$$

for a given leg i. Provided that the joints are perfectly rigid in all directions but one, that the links are perfectly rigid and that the geometry of the robotic manipulator is known exactly, we have

$$\mathbf{P} = \mathbf{P}_1 = \mathbf{P}_2 = \mathbf{P}_3. \tag{19}$$

However, if we consider small clearances in all the joints, we must include small errors in Eq. (18) of $\mathbf{P}_i$ for Eq. (19) to hold true.

C. Joint-Clearance Errors

These small errors may be represented by six-dimensional small-displacement screws, as was done in [10]–[12]. Taking into account clearances in the joints, the frame $\mathscr{F}_{i,j}$ associated with link j of leg i is shifted to $\mathscr{F}'_{i,j}$. Provided it is small, this error on the pose of joint $j+1$ with respect to joint j may be represented by the small-displacement screw

$$\delta\mathbf{s}_{i,j} \equiv \begin{bmatrix} \delta\mathbf{r}_{i,j} \\ \delta\mathbf{t}_{i,j} \end{bmatrix} \in \mathbb{R}^6, \tag{20}$$

where $\delta\mathbf{r}_{i,j} \in \mathbb{R}^3$ represents the small rotation taking frame $\mathscr{F}_{i,j}$ onto $\mathscr{F}'_{i,j}$, while $\delta\mathbf{t}_{i,j} \in \mathbb{R}^3$ points from the origin of $\mathscr{F}_{i,j}$ to that of $\mathscr{F}'_{i,j}$. $\delta\mathbf{s}_{i,j}$ can also represented as the 4×4 matrix

$$\delta\mathbf{S}_{i,j} = \begin{bmatrix} \delta\mathbf{R}_{i,j} & \delta\mathbf{t}_{i,j} \\ \mathbf{0}_3^T & 0 \end{bmatrix} \in \mathrm{se}(3), \tag{21}$$

where $\delta\mathbf{R}_{i,j} \equiv \partial(\delta\mathbf{r}_{i,j}\times\mathbf{x})/\partial\mathbf{x}$ is the cross-product matrix of $\delta\mathbf{r}_i$.

D. Error on the Moving-Platform Pose

Because of joint clearances, the frame $\mathscr{P}_i$ is shifted to $\mathscr{P}'_i$. In SE(3), the displacement taking frame $\mathscr{F}_{i,j}$ onto $\mathscr{F}'_{i,j}$ is given by the matrix exponential of $\delta\mathbf{S}_{i,j}$, $e^{\delta\mathbf{S}_{i,j}}$. As a result, the screw that represents the pose of the shifted moving-platform may be computed through the i^{th} leg as

$$\mathbf{P}'_i = \prod_{j=1}^{3} e^{\delta\mathbf{S}_{i,j}}\mathbf{S}_{i,j}, \tag{22}$$

where screw $\mathbf{P}'_i$ takes frame $\mathscr{F}_{i,1}$ onto $\mathscr{P}'_i$ when taking errors into account. In order to obtain the moving-platform pose error, the screw $\Delta\mathbf{P}_{i_{|\mathscr{P}_i}}$ that takes the nominal moving-platform pose $\mathscr{P}_i$ onto the shifted one $\mathscr{P}'_i$ through the i^{th} leg is expressed in frame $\mathscr{P}_i$ as

$$\Delta\mathbf{P}_{i_{|\mathscr{P}_i}} = \mathbf{P}_i^{-1}\mathbf{P}'_i, \tag{23}$$

$$= \prod_{j=3}^{1}\mathbf{S}_{i,j}^{-1}\prod_{j=1}^{3}\left(e^{\delta\mathbf{S}_{i,j}}\mathbf{S}_{i,j}\right), \tag{24}$$

$$\approx \mathbf{1}_{4\times4} + \sum_{j=1}^{3}\left(\prod_{k=3}^{j}\mathbf{S}_{i,k}^{-1}\delta\mathbf{S}_{i,j}\prod_{l=j}^{3}\mathbf{S}_{i,l}\right). \tag{25}$$

From Eq. (25), we see that end-effector displacement $\Delta\mathbf{P}_{i_{|\mathscr{P}_i}}$ is small, since it is composed of the identity matrix plus a finite sum of small-displacement screws. Therefore, $\Delta\mathbf{P}_{i_{|\mathscr{P}_i}}$ may be as well represented with the small displacement screw

$$\delta\mathbf{P}_{i_{|\mathscr{P}_i}} = \sum_{j=1}^{3}\left(\prod_{k=3}^{j}\mathbf{S}_{i,k}^{-1}\delta\mathbf{S}_{i,j}\prod_{l=j}^{3}\mathbf{S}_{i,l}\right). \tag{26}$$

Alternatively, the small-displacement screw taking frame $\mathscr{P}_i$ onto frame $\mathscr{P}'_i$ may be computed as a vector in $\mathbb{R}^6$, namely, $\delta\mathbf{p}_{i_{|\mathscr{P}_i}}$. To this end, let us recall that the adjoint map of screw $\mathbf{S}_{i,j}$ is

$$\mathrm{adj}(\mathbf{S}_{i,j}) \equiv \begin{bmatrix} \mathbf{R}_{i,j} & \mathbf{O}_{3\times3} \\ \mathbf{T}_{i,j}\mathbf{R}_{i,j} & \mathbf{R}_{i,j} \end{bmatrix}, \tag{27}$$

where $\mathbf{T}_{i,j} \equiv \partial(\mathbf{t}_{i,j}\times\mathbf{x})/\partial\mathbf{x}$ is the cross-product matrix of $\mathbf{t}_{i,j}$. Then, we may express $\delta\mathbf{s}_{i,j}$ in frame $\mathscr{F}_{i,j+1}$ by simply computing $\mathrm{adj}(\mathbf{S}_{i,j}^{-1})\delta\mathbf{s}_{i,j}$. As a result, $\delta\mathbf{s}_{i,j}$ may be expressed in frame $\mathscr{P}_i$ through the product

$$\left(\prod_{k=3}^{j}\mathrm{adj}(\mathbf{S}_{i,k}^{-1})\right)\delta\mathbf{s}_{i,j}, \tag{28}$$

and the small-displacement screw taking $\mathscr{P}_i$ onto $\mathscr{P}'_i$ simply becomes

$$\delta\mathbf{p}_{i_{|\mathscr{P}_i}} = \sum_{j=1}^{3}\prod_{k=3}^{j}(\mathrm{adj}(\mathbf{S}_{i,k}))^{-1}\delta\mathbf{s}_{i,j} \tag{29}$$

It is noteworthy that $\delta\mathbf{p}_{i_{|\mathscr{P}_i}}$ is expressed in the frame attached to the moving platform, i.e., $\mathscr{P}_i$. For the evaluation of the pose errors on the moving-platform, the small-displacement screw taking $\mathscr{P}_i$ onto $\mathscr{P}'_i$ has to be expressed in the reference attached to the fixed base, i.e., $\mathscr{F}_b$. Let $\delta\mathbf{p}_{i_{|\mathscr{F}_b}}$ be this small-displacement screw expressed in $\mathscr{F}_b$:

$$\delta\mathbf{p}_{i_{|\mathscr{F}_b}} = \prod_{j=0}^{3}(\mathbf{N}_{i,j})\delta\mathbf{p}_{i_{|\mathscr{P}_i}}, \tag{30}$$

where

$$\mathbf{N}_{i,j} \equiv \begin{bmatrix} \mathbf{R}_{i,j} & \mathbf{O}_{3\times3} \\ \mathbf{O}_{3\times3} & \mathbf{R}_{i,j} \end{bmatrix}. \tag{31}$$

$\mathbf{N}_{i,0}$ being used to express $\mathscr{F}_{i,1}$ into $\mathscr{F}_b$. As a result,

$$\delta\mathbf{p}_{i_{|\mathscr{F}_b}} = \prod_{j=0}^{3}\mathbf{N}_{i,j}\sum_{j=1}^{3}\prod_{k=3}^{j}\left(\mathrm{adj}(\mathbf{S}_{i,k})\right)^{-1}\delta\mathbf{s}_{i,j} \tag{32}$$

$$= \sum_{j=1}^{3}\left(\prod_{l=0}^{3}\mathbf{N}_{i,l}\prod_{k=3}^{j}(\mathrm{adj}(\mathbf{S}_{i,k}))^{-1}\delta\mathbf{s}_{i,j}\right) \tag{33}$$

The following compact form may be used:

$$\delta\mathbf{p}_{i_{|\mathscr{F}_b}} = \mathbf{M}_i\delta\mathbf{s}_i, \tag{34}$$

where

$$\mathbf{M}_i \equiv \begin{bmatrix}\mathbf{M}_{i,1} & \mathbf{M}_{i,2} & \mathbf{M}_{i,3}\end{bmatrix}, \tag{35}$$

$$\mathbf{M}_{i,j} \equiv \prod_{l=0}^{3}(\mathbf{N}_{i,l})\prod_{k=3}^{j}(\mathrm{adj}(\mathbf{S}_{i,k}))^{-1}, \tag{36}$$

$$\delta\mathbf{s}_i \equiv \begin{bmatrix}\delta\mathbf{s}_{i,1}^T & \delta\mathbf{s}_{i,2}^T & \delta\mathbf{s}_{i,3}^T\end{bmatrix}^T. \tag{37}$$

E. Modeling the clearances in a prismatic joint

Intuitively, clearances in a joint are best modeled by bounding its associated errors below and above. Assuming that the lower and upper bounds are the same, this generally yields six parameters that bound the error screw $\delta\mathbf{s}_{i,j}$. Figure 6 illustrates a clearance-affected prismatic joint. Likewise, a clearance-affected revolute joint is shown in [14]. Recall that frame $\mathscr{F}_{i,j}$ is attached to joint j of leg i according to the Denavit-Hartenberg convention. As a result, its Z-axis is aligned with the prismatic-joint axis. Moreover, the origin of $\mathscr{F}_{i,j}$ may be chosen to lie at the centroid of the prismatic joint as shown in Fig. 6. In this case, the Z

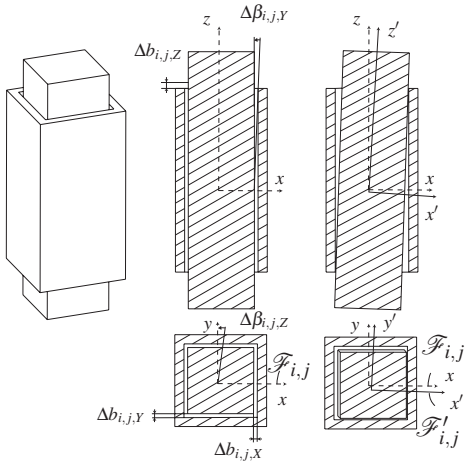

Fig. 6. Clearance-affected prismatic joint

components of $\delta\mathbf{r}_{i,j}$ and $\delta\mathbf{t}_{i,j}$—both defined in Eq. (20)—are axial components, while the X and Y components are radial. Accordingly, the error bounds are written as

$$\begin{aligned}
&\delta r_{i,j,X}^2 \le \Delta\beta_{i,j,X}^2, \delta r_{i,j,Y}^2 \le \Delta\beta_{i,j,Y}^2\\
&\delta r_{i,j,Z}^2 \le \Delta\beta_{i,j,Z}^2,\\
&\delta t_{i,j,X}^2 \le \Delta b_{i,j,X}^2, \delta t_{i,j,Y}^2 \le \Delta b_{i,j,Y}^2,\\
&\delta t_{i,j,Z}^2 \le \Delta b_{i,j,Z}^2,
\end{aligned}$$

where $\delta\mathbf{r}_{i,j} \equiv [\delta r_{i,j,X} \quad \delta r_{i,j,Y} \quad \delta r_{i,j,Z}]^T$ and $\delta\mathbf{t}_{i,j} \equiv [\delta t_{i,j,X} \quad \delta t_{i,j,Y} \quad \delta t_{i,j,Z}]^T$.

F. The maximum moving-platform pose errors

Formally, the maximum moving-platform point-displacement $p_{\max}$ due to joint clearances is obtained by solving the problem

$$\begin{aligned}
-p_{\max}^2 \equiv \text{minimize} \quad & -\sum_{k=4,5,6} (\mathbf{e}_{6,k}^T \delta\mathbf{p})^2, \qquad (38)\\
\text{over} \quad & \delta\mathbf{p},\ \delta\mathbf{s}_{i,j},\ j=1,\ldots,3,\ i=1,\ldots,3,\\
\text{subject to} \quad & (\mathbf{e}_{6,1}^T \delta\mathbf{s}_{i,j})^2 - \Delta\beta_{X,i,j}^2 \le 0,\\
& (\mathbf{e}_{6,2}^T \delta\mathbf{s}_{i,j})^2 - \Delta\beta_{Y,i,j}^2 \le 0,\\
& (\mathbf{e}_{6,3}^T \delta\mathbf{s}_{i,j})^2 - \Delta\beta_{Z,i,j}^2 \le 0,\\
& (\mathbf{e}_{6,4}^T \delta\mathbf{s}_{i,j})^2 - \Delta b_{X,i,j}^2 \le 0,\\
& (\mathbf{e}_{6,5}^T \delta\mathbf{s}_{i,j})^2 - \Delta b_{Y,i,j}^2 \le 0,\\
& (\mathbf{e}_{6,6}^T \delta\mathbf{s}_{i,j})^2 - \Delta b_{Z,i,j}^2 \le 0,\\
& \delta\mathbf{p} = \mathbf{M}_i \delta\mathbf{s}_i,\\
& j=1,\ldots,3,\ i=1,\ldots,3,
\end{aligned}$$

where $\mathbf{e}_{j,k} \in \mathbb{R}^6$ is defined such that $\mathbf{1}_{j\times j} \equiv [\mathbf{e}_{j,1} \quad \mathbf{e}_{j,2} \quad \cdots \quad \mathbf{e}_{j,j}]$. The expression of the maximum rotation $r_{\max}$ of the moving-platform due to joint clearances is the same as that of $p_{\max}$, except for the objective function and the constraint number, namely,

$$\begin{aligned}
-r_{\max}^2 \equiv \text{minimize} \quad & -\sum_{k=1,2,3} (\mathbf{e}_{6,k}^T \delta\mathbf{p})^2, \qquad (39)\\
\text{over} \quad & \delta\mathbf{p},\ \delta\mathbf{s}_{i,j},\ j=1,\ldots,3,\ i=1,\ldots,3,\\
\text{subject to} \quad & (\mathbf{e}_{6,1}^T \delta\mathbf{s}_{i,j})^2 - \Delta\beta_{X,i,j}^2 \le 0,\\
& (\mathbf{e}_{6,2}^T \delta\mathbf{s}_{i,j})^2 - \Delta\beta_{Y,i,j}^2 \le 0,\\
& (\mathbf{e}_{6,3}^T \delta\mathbf{s}_{i,j})^2 - \Delta\beta_{Z,i,j}^2 \le 0,\\
& \delta\mathbf{p} = \mathbf{M}_i \delta\mathbf{s}_i,\\
& j=1,\ldots,3,\ i=1,\ldots,3,
\end{aligned}$$

In the scope of this paper, optimization problems (38) and (39) are solved with ModeFrontier software [13]. This optimization problem can also be solved by means of Interval Analysis [14] and with the algorithm proposed in [15].

V. COMPARISON OF TWO 3-PPR PPMS

This section deals with the evaluation of the sensitivity of the moving platform pose to joint clearances for the two PPMs defined in Sec. III-B. The error bounds characterizing the joint clearances and defined in Sec. IV-E are supposed to be equal to:

$$\begin{aligned}
\Delta\beta_{i,1,X} &= \Delta\beta_{i,1,Y} = \Delta\beta_{i,1,Z} = 0.01 \text{ rad},\\
\Delta b_{i,1,X} &= \Delta b_{i,1,Y} = 0.1 \text{ mm},\\
\Delta b_{i,1,Z} &= 0,\\
\Delta\beta_{i,2,X} &= \Delta\beta_{i,2,Y} = \Delta\beta_{i,2,Z} = 0.01 \text{ rad},\\
\Delta b_{i,2,X} &= \Delta b_{i,2,Y} = \Delta b_{i,2,Z} = 0.05 \text{ mm},\\
\Delta\beta_{i,3,XY} &= 0.01 \text{ rad},\\
\Delta\beta_{i,3,Z} &= 0,\\
\Delta b_{i,3,XY} &= \Delta b_{i,3,Z} = 0.1 \text{ mm}.
\end{aligned}$$

Figures 7 and 8 show the isocontours of the maximum point-displacement $p_{\max}$ throughout the workspace of the 3-PPR PPMs with a U- and a Δ-shape base for two rotation angles of their moving platform. It appears that the maximum orientation error of their moving-platform is constant and equal to 0.011 rad throughout the manipulator workspace for both the U and the Δ-shape base and any rotation angle of the moving-platform. Table III gives $r_{\max}$ and the maximum and minimum values of $p_{\max}$ corresponding to those isocontours. It appears that $p_{\max}$ are slightly higher for the PPM with a U-shape base than for the PPM with the Δ-shape base. Nevertheless, from Sec. III-B, the workspace of the former is quite larger than the workspace of the latter. For instance, for a rotation angle of the moving platform equal to $\pi/6$,

TABLE III

MAXIMUM AND MINIMUM VALUES OF $p_{\max}$ AND $r_{\max}$

	U-shape $\phi=\pi/6$	U-shape $\phi=\pi/2$	Δ-shape $\phi=\pi/6$	Δ-shape $\phi=\pi/2$
min($p_{\max}$) [mm]	0.18	0.38	0.34	0.38
max($p_{\max}$) [mm]	0.44	0.63	0.40	0.44
$r_{\max}$ [rad]	0.011	0.011	0.011	0.011

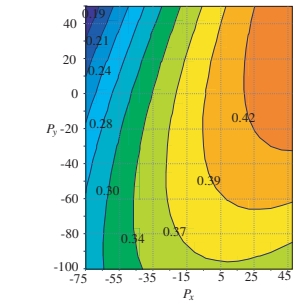

(a)

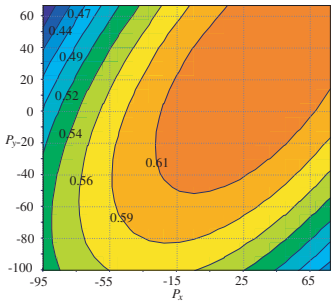

(b)

Fig. 7. 3-PPR PPM with a U-shape base: isocontours of the maximum point-displacement $p_{\max}$ throughout WS in [mm]: (a) $\phi = \pi/6$, (b) $\phi = \pi/2$

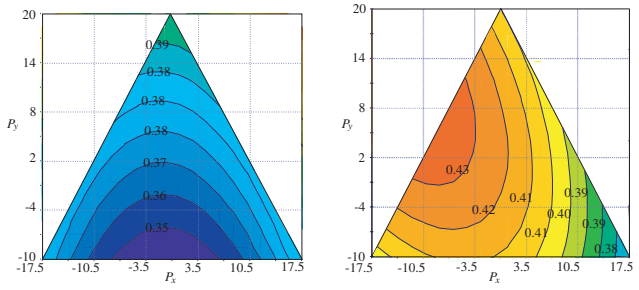

(a) (b)

Fig. 8. 3-PPR PPM with a Δ-shape base: isocontours of the maximum point-displacement $p_{\max}$ throughout WS in [mm]: (a) $\phi = \pi/6$, (b) $\phi = \pi/2$

the workspace size of the 3-PPR PPM with a U-shape base is about thirty times larger than the workspace size of its counterpart with a Δ-shape base while the maximum values of $p_{\max}$ for the former are only 5% higher than for the latter.

VI. CONCLUSIONS

In this paper, 3-PPR planar parallel manipulators with Δ- or U-shape base were compared with respect to their workspace size and kinematic sensitivity to joint clearances. An error prediction model applicable to both serial and parallel manipulators was developed. As a result, two non-convex quadratically constrained quadratic programs were formulated in order to find the maximum reference-point position error and the maximum orientation error of the moving-platform for given joint clearances. It appears that the workspace of a 3-PPR planar parallel manipulator with a U-shape base is quite larger than the one of a 3-PPR planar parallel manipulator with a Δ-shape for given prismatic joint limits. However, the latter is slightly better than the former in terms of kinematic sensitivity to joint clearances. Finally, those results will be checked experimentally with a real prototype in a future work.

REFERENCES

[1] C.M. Gosselin and J. Angeles, "The optimum kinematic design of a planar three-degree-of-freedom parallel manipulator". *Journal of mechanisms, transmissions, and automation in design*, vol. 110(1), 1988, pp 35–41.

[2] R. Ur-Rehman, S. Caro, D. Chablat and P. Wenger, "Multiobjective design optimization of 3PRR planar parallel manipulators", *in 20th CIRP Design Conference*, Nantes, France, 2010.

[3] I.A. Bonev, D. Zlatanov and C.M. Gosselin, "Singularity analysis of 3-dof planar parallel mechanisms via screw theory", *ASME J. of Mechanical Design*, vol. 125(3), 2003, pp 573–581.

[4] J.A. Carretero, I. Ebrahimi and R. Boudreau, *Advances in Robot Kinematics: Analysis and Design*, chapter A Comparison between Two Motion Planning Strategies for Kinematically Redundant Parallel Manipulators, pages 243–252, Springer Netherlands, 2008.

[5] J.-P. Merlet, "Direct kinematics of planar parallel manipulators", *IEEE Int. Conf. on Robotics and Automation*, Minneapolis, 1996, pp 3744–3749.

[6] S. Bai and S. Caro, "Design and Analysis of a 3-PPR Planar Robot with U-shape Base", *in 14th International Conference on Advanced Robotics*, Munich, Germany, June 22-26, 2009.

[7] J. Carusone and G.M. D'Eleuterio, "Tracking control for end-effector position and orientation of structurally flexible manipulators", *Journal of Robotic Systems*, vol. 10(6), 1993, pp 847–870.

[8] H. Zhuang, "Self-calibration of parallel mechanisms with a case study on stewart platforms", *IEEE Transactions on Robotics and Automation*, vol. 13(3), 1997, pp 387–397.

[9] R. Hartenberg and J. Denavit, *Kinematic Synthesis of Linkages*, McGraw-Hill, New York, 1964.

[10] H.S. Wang and B. Roth, "Position errors due to clearances in journal bearings", *ASME Journal of Mechanisms, Transmissions, and Automation in Design*, vol. 111(3), 1989, pp 315–320.

[11] S. Venanzi and V. Parenti-Castelli, "A new technique for clearance influence analysis in spatial mechanisms", *ASME Journal of Mechanical Design*, vol. 127(3), 2005, pp 446–455.

[12] J. Meng, D. Zhang and Z. Li, "Accuracy analysis of parallel manipulators with joint clearance", *ASME Journal of Mechanical Design*, vol. 131(1), 2009, pp 011013–1–011013–9.

[13] ESTECO. modefrontier. `http://www.esteco.it`.

[14] N. Berger, R. Soto, A. Goldsztejn, S. Caro and P. Cardou, "Finding the maximal pose error in robotic mechanical systems using constraint programming", *In The Twenty Third International Conference on Industrial, Engineering and Other Applications of Applied Intelligent Systems* – IEA-AIE, 2010.

[15] K.L. Hoffman, "Method for globally minimizing concave functions over convex sets", *Mathematical Programming*, vol. 20(1), 1981, pp 22–32.